SSRG International Journal of Electrical and Electronics Engineering
ISSN: 2348-8379/ https://doi.org/10.14445/23488379/IJEEE-V12I10P102

Volume 12 Issue 10, 13-20, October 2025

Original Article

Analysis of Impact of Electric Arc Furnace on Power Quality and Its Mitigation with MMC

Gajendran Alagupandi[1], Thirumalai Vasan R[2]

[1,2]*Vellore Institute of Technology University, Vellore, India*

[2]*Corresponding Author : thirumalai.r@vit.ac.in*

Received: 02 August 2025 Revised: 04 September 2025 Accepted: 03 October 2025 Published: 30 October 2025

Abstract *- The paper investigates a closed-loop control algorithm for a Modular Multi-Level Converter-based system in the elimination of harmonics, mitigation of voltage imbalance, reactive and active power compensation, and improving the power quality of a grid having an Electric Arc Furnace as load. The submodule voltages are balanced to reduce stress on semiconductors and prevent module saturation. The effectiveness of the system is analyzed with a MATLAB/SIMULINK-based simulation. Simulation results indicate mitigation of current harmonics and flicker reduction with MMC.*

Keywords *- Active Power, Capacitor voltage balancing, Electric Arc furnace, Flicker, MMC, Reactive Power.*

1. Introduction

Electrical Arc Furnaces (EAFs) have been commonly used to melt iron and scrap metal. The process of melting the metals is achieved by supplying large amounts of electrical energy to the interior of the furnace with the help of graphite electrodes. Initially, medium voltage is applied to melt lighter metal scraps, and then high voltage is applied to these electrodes, which produce electric arcs providing heat to the melting operation. Due to the unstable nature of these arcs, the magnitude of the current varies over a wide range. As the melting process continues and input power increases, the process becomes more stable, but the current can still contain fluctuations of low frequencies [1].

Therefore, Electric Arc Furnaces are nonlinear loads with a time-variant nature, which leads to issues like voltage flicker, random change in power levels, harmonics, and unbalanced voltage and current. The reason for asymmetry in these arc furnaces is as follows:

1. Unequal impedance of each phase of the electric arc furnace
2. The change in arc resistance is due to the change in the length of the arc during the melting process.

MMC is a voltage-source converter that uses multiple identical and independently controllable submodules to generate a high-quality, stepped approximation of a sine wave. An electrical arc furnace is generally one of the largest loads present in the industrial grid. So, it is necessary that the disturbances caused by it should be minimized to reduce its effects on other loads connected to the grid [2].

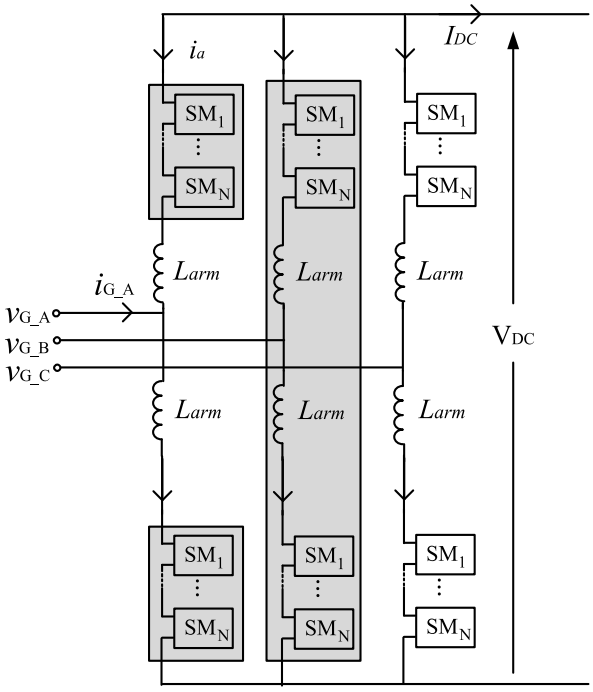

Fig. 1 Model of MMC with multiple submodules [10]

Many techniques have been proposed to mitigate the disturbances produced by the EAF. This paper analyses the effect of the MMC (Modular Multilevel Converter) based Active Power Filter in improving the power factor by cancelling out the harmonics and minimising voltage imbalance [3]. Comparison between the SVC (Static VAR Compensator based on Thyristor) based solution vs the MMC based solution for the Electric Arc furnace shown below;

Table 1 . MMC vs SVC

Feature	MMC	SVC
Control Speed	High	Medium
Reactive Power Compensation	Dynamic	Sluggish
Active Power Compensation	Yes	No
Harmonic Mitigation	Yes, less THD	Requires passive filters
Flicker Reduction	High	Medium
Modularity & Scalability	Modular and scalable	Fixed design

Out of all multilevel converter topologies, MMC has been widely accepted as the choice of STATCOM because of its strong fault-clearing capacity and scalability from medium to high voltage applications [4]. The reduced power rating of each semiconductor switch makes it suitable for high-power applications [5]. The MMCs provide harmonics reduction with low switching frequency and flexible design. On the DC side, the voltage level has been maintained via capacitors present in each submodule of the MMC. The control methodology deployed ensures that the DC voltage is maintained at the sub-module level and the converter level by ensuring a balance in each capacitor's voltage. The modules are selected to be inserted or bypassed based on their charging level and the direction of flow of current in the arm. The choice of submodules to be inserted is based on a sorting algorithm like Bubble Sort [6]. However, this leads to complexities and requires more computational resources as the number of submodules increases. This paper explores the Capacitor Voltage Mapping Strategy, which reduces execution time by making use of memory blocks for storing submodule state in the arm of MMC.

2. System Configuration

2.1. Modelling of Arc Furnace

An arc furnace's operation could be divided into three phases for its electrical modelling [7].

2.1.1. Reignition

Following its extinguishment, the arc begins the process of reignition. Arc voltage goes up from zero until arc current exceeds the zero-crossing point. Until arc voltage exceeds reignition voltage, a small leakage current emerges at this stage [7]. At this point, the equivalent circuit functions as an open circuit. The reignition voltage is directly proportional to the length of the arc.

2.1.2. Arc Established

Once the reignition voltage is reached, the arc becomes fully established. This transition is accompanied by a transient phenomenon in the voltage waveform, observed at the very beginning of the arc melting process. During this transient phase, the arc voltage experiences a sudden drop from the reignition voltage [8].

2.1.3. Arc Extinction

During the extinction process, the established arc approaches its end. The arc voltage exhibits a continuous and smooth decrease at first, but experiences a sharper decline after arc extinguishment.

For this study, MATLAB/SIMULINK is used to replicate the Electric Arc Furnace using three controlled voltage sources for each phase of a network. The VI characteristics of the controlled voltage source are hyperbolic in nature and are governed by equations 1 and 2 [9].

$$V(i) = V_t + \frac{P_a}{(I_a+i)} sgn(i) \quad (1)$$

Here, i represent the load current

V(i) represents the voltage across the arc furnace load as a function of load current.

V_t is the threshold voltage of arc length

P_a is arc power

I_a is arc current

The value of the signum function can be given below:

$$sgn(x) = \begin{cases} -1 & x \le 0 \\ +1 & x \ge 0 \end{cases} \quad (2)$$

An effect of voltage flicker has been simulated with the help of the threshold voltage.

$$V_t = V_r[1 + m \times sin(\omega t)] \quad (3)$$

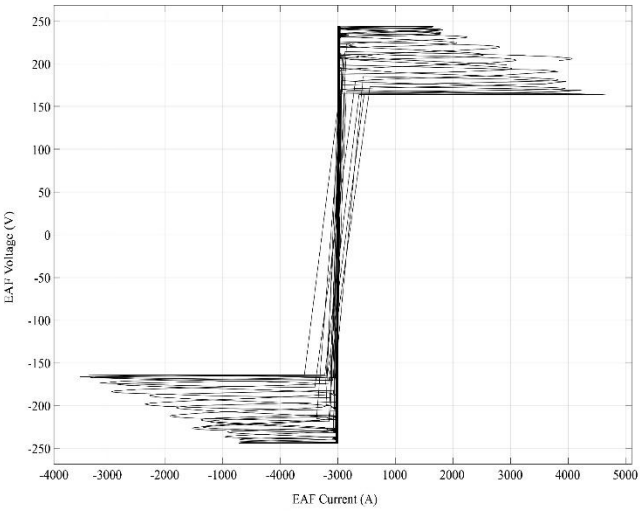

Fig. 2 V-I characteristics of electric arc furnace

Here,

ω = flicker frequency

V_r = base reference voltage without any arc m is the modulation index

The non-linear V-I characteristics of EAFs' load, as illustrated in Figure 2, are a cause of their polluting nature. The resultant model simplifies the operating mechanism of EAF by neglecting the voltage rise time, which leads to an abrupt change in arc voltage when the arc current is near the zero crossing.

2.2. Design of Modular Multilevel Converter

The MMC comprises multiple power modules arranged in sequence. Each power module comprises a half-bridge and one capacitor on the DC side, as illustrated in Figure 3. The converter block is modelled using IGBT and diode pairs. The two IGBTs are complementary switches; therefore, when one is in the ON state, the other one must be in the OFF state. The PWM generator provides the firing pulses that activate the converter's switching.

A three-phase MMC contains 3 upper arms and 3 lower arms for each phase of the system. Every arm contains multiple cascaded submodules as shown in Figure 1. Half-bridge topology has been used due to its low semiconductor losses, simplicity, and lower costs [11]. As seen in Figure 1, arm current flows continuously because of the presence of coupling inductors, which avoids the high magnitude di/dt during the VSC switching [12]. The presence of multiple modules leads to smaller fault currents in the DC side and lower stress per semiconductor. The complexity of the design does not increase with the number of levels employed, and each module could be turned ON/OFF for maintenance.

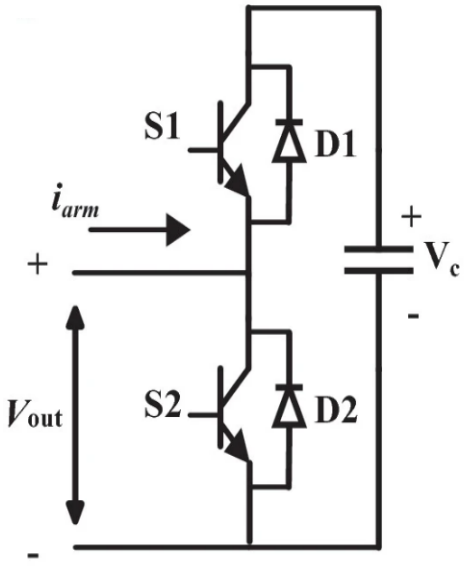

Fig. 3 Half bridge configuration of MMC submodules [10]

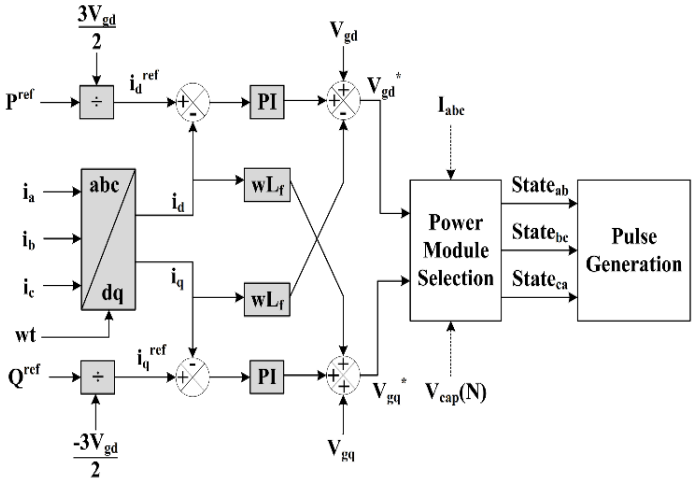

Fig. 4 Active and reactive power compensation control mechanism

The MMC-based converter has been connected in parallel to the grid and the load. The grid operates in a balanced condition with voltage or current as follows:

$$V_{ga} = \sqrt{2}Vsin(w_o t) \quad (4)$$

$$V_{gb} = \sqrt{2}Vsin\left(w_o t - \frac{2\pi}{3}\right) \quad (5)$$

$$V_{gc} = \sqrt{2}Vsin\left(w_o t + \frac{2\pi}{3}\right) \quad (6)$$

$$I_{ga} = \sqrt{2}Isin(w_o t - \phi) \quad (7)$$

$$I_{gb} = \sqrt{2}Isin\left(w_o t - \frac{2\pi}{3} - \phi\right) \quad (8)$$

$$I_{gc} = \sqrt{2}Isin\left(w_o t + \frac{2\pi}{3} - \phi\right) \quad (9)$$

3. MMC Control Mechanism

The STATCOM is a variable current source connected in parallel with the grid at PCC through an isolating transformer.

A closed-loop current control approach has been employed to inject the necessary current for active and reactive power adjustments.

3.1. Active and Reactive Power Control

The quantity of active or reactive power delivered to the system could be controlled via inputs Pref and Qref [13]. This is denoted in the equations below,

$$P = \frac{3}{2} V_{gd} i_{gd} + V_{gq} i_{gq} \tag{10}$$

$$Q = \frac{3}{2} V_{gd} i_{gd} - V_{gq} i_{gq} \tag{11}$$

During the control of the system, the PLL is synchronised to the grid voltage; therefore, the q component of voltage in the above equations is set to zero. Therefore, P and Q can be denoted as,

$$P = \frac{3}{2} V_{gd} i_{gd} \tag{12}$$

$$Q = \frac{3}{2} V_{gd} i_{gd} \tag{13}$$

The control loop of the system is illustrated in Figure 4. Active or reactive power flowing into the arc furnace is taken as input.

After the process of converting the inputs into per-unit terms, the power invariant version of the Park Transform is applied to the load current to convert it into the D-Q frame [14]. This D-Q transform is carried out by taking the PCC voltage V_{pcc} , as a synchronization reference.

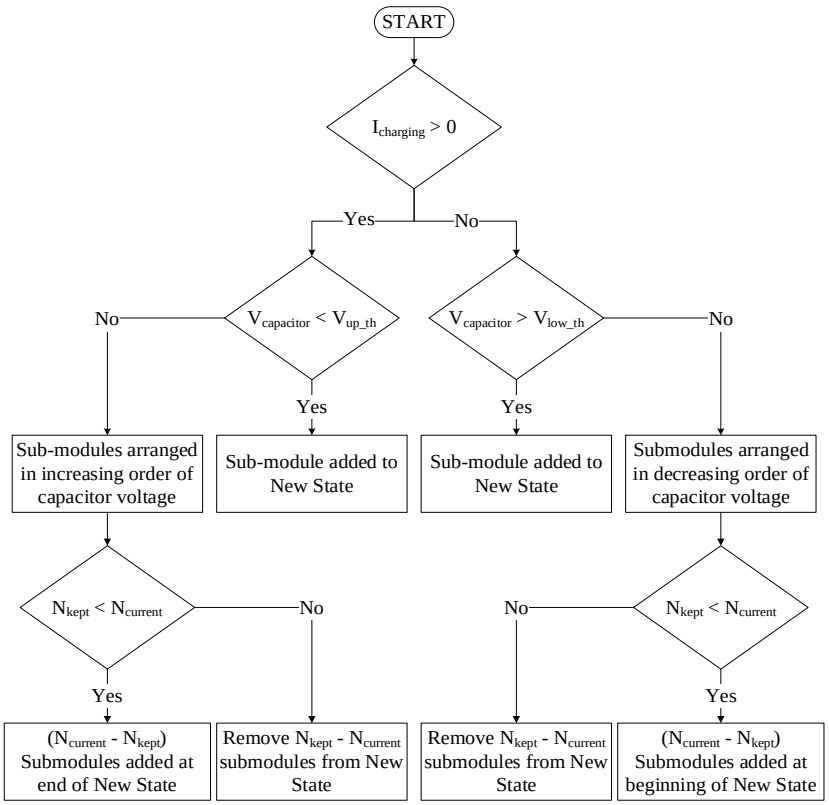

Fig. 5 Capacitor voltage balancing algorithm

Considering Vp,n to be the converter voltage, the current through each phase of the system can be expressed as:

$$L \frac{d}{dt} I_{ua}(t) = -V_{ua}(t) - V_{ga}(t) \tag{14}$$

$$L \frac{d}{dt} I_{la}(t) = -V_{la}(t) - V_{ga}(t) \tag{15}$$

The PQ control is achieved using the direct control method. Implementing the Park transform on the above equations:

$$\begin{bmatrix} I_{d-ref} \\ I_{q-ref} \\ I_{o-ref} \end{bmatrix} = [K_p] \begin{bmatrix} I_{ga} \\ I_{gb} \\ I_{gc} \end{bmatrix} \tag{16}$$

Where, K_p is given as:

$$\left[\frac{2}{3}\right] \begin{bmatrix} cos\ \omega t & cos\left(\omega t - \frac{2\pi}{3}\right) & cos\left(\omega t + \frac{2\pi}{3}\right) \\ -sin\ \omega t & -sin\left(\omega t - \frac{2\pi}{3}\right) & sin\left(\omega t + \frac{2\pi}{3}\right) \\ \frac{1}{2} & \frac{1}{2} & \frac{1}{2} \end{bmatrix} \tag{17}$$

$$V_{ul-d} = L\frac{d}{dt}i_{d-ref} - wLi_{q-ref} + V_{gd} \quad (18)$$

$$V_{ul-q} = L\frac{d}{dt}i_{q-ref} + wLi_{d-ref} + V_{gq} \quad (19)$$

3.2. Voltage Balancing Control of Capacitor

Submodules are inserted and bypassed to provide voltage balancing in capacitors. When a submodule is introduced, the capacitors are either charged or discharged based on the current's flow direction. If a submodule is circumvented, the voltage across the capacitor is maintained. This process is explained in Figure 5. A voltage tolerance zone [$V_{up\text{-}th}$-$V_{low\text{-}th}$] is defined for the capacitors; this zone determines whether the module is sufficiently charged or not [15].

$$\boldsymbol{V_{up-th} = (1+\mu) \times mean(Vc_{current})} \quad (20)$$

$$\boldsymbol{V_{low-th} = (1-\mu) \times mean(Vc_{current})} \quad (21)$$

If the current is charging modules, then the capacitors with voltage below the upper limit of $V_{up\text{-}th}$ are eligible to be activated. If the current is discharging the modules, then the capacitors having voltage exceeding the tolerance limit $V_{low\text{-}th}$ are activated, ensuring sufficient energy reserves during discharge [16]. The algorithm maintains a desired number of activated modules ($N_{current}$). If modules already activated fall within the desired range ($N_{kept} = N_{current}$), no further changes are made. In case of underactivation of modules, additional modules are needed ($N_{kept} < N_{current}$). The remaining modules are sorted based on their voltage relative to the tolerance voltages. In case the submodules are being charged, they are arranged in ascending order for charging, prioritizing modules closest to the target voltage for activation. If the submodules are being discharged, then they are arranged in descending order for discharging; this prioritizes modules with the highest remaining charge for activation. This process is carried out until the desired number ($N_{current}$) is reached [17]. If modules are overactivated, the algorithm randomly selects modules from the currently activated pool to deactivate them. The deactivation continues until the desired number of activated modules (Ncurrent) remains. This random module selection for deactivation during over-activation ensures fair utilization of all modules over time. The technique used is capacitor voltage mapping, which uses a combination of memory blocks to "Remember" the old charging state of capacitors, and a round robin method to ensure that a single capacitor is not overused.

3.3. Pulse Generation

The output of the Power Selection module controls the pulse generation process for the MMC. The pulse generation logic is described in Table 2.

Table 2. Pulse generation of the converter

Condition	State	Ig	Submodule Capacitor
0	Pulse Blocked	-	Capacitor disconnected
1	V{g} shorted	-	Capacitor disconnected
2	{g} shorted	-	Capacitor disconnected
3	V{g} +ve	Positive	Capacitor disconnected
3	V{g} +ve	Negative	Capacitor charging
4	V{g} -ve	Positive	Capacitor charging
4	V{g} -ve	Negative	Capacitor disconnected

4. Simulation Results

The system described above is simulated and analysed on the MATLAB / Simulink platform. The overview of the system can be seen in Figure 6. The Non-Linear Load subsystem consists of the Electric Arc Furnace, Diode Bridge Rectifiers, and other loads consuming reactive power from the grid. The weak grid has been supported by an MMC connected in parallel to the loads.

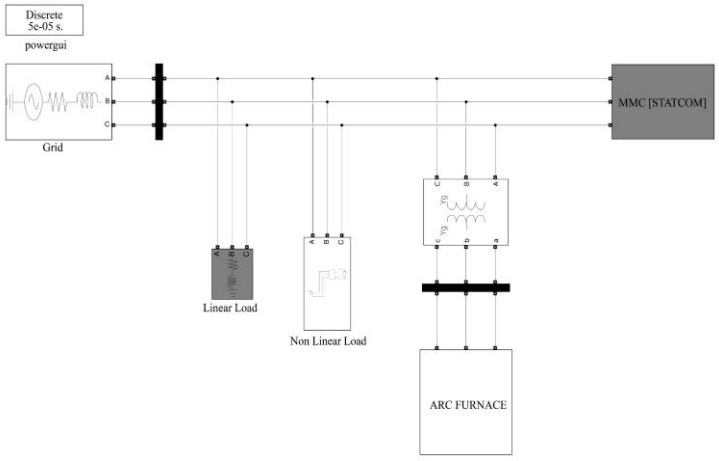

Fig. 6 Overview of the simulated system

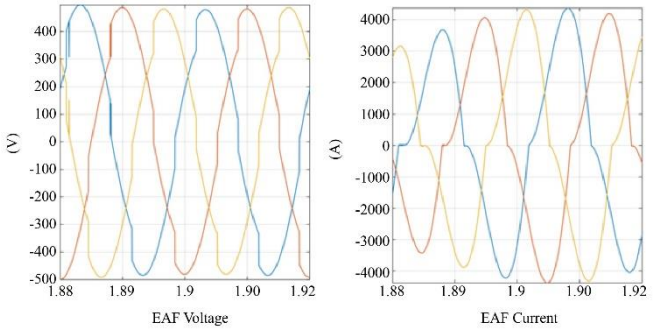

Fig. 7 Electric Arc Furnace Voltage and Current

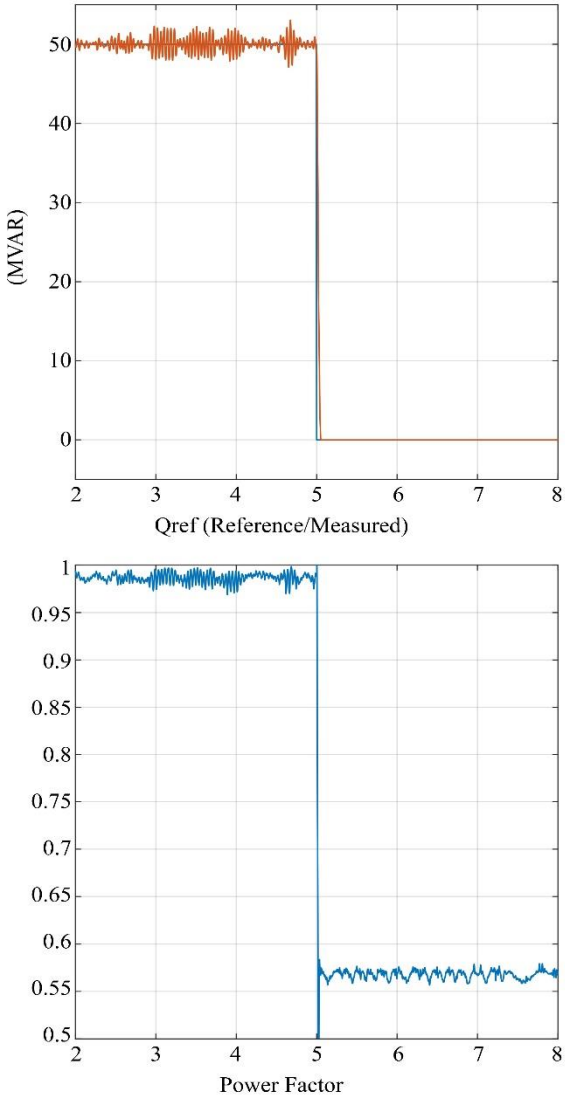

Fig. 8 Reactive power, Power factor

The Arc Furnace has been modelled by using a controlled voltage source, with the reference voltage being provided using Equations 1-3. As the EAF has been modelled as a non-ohmic load, it is observed from Figure 7 that the load current is unbalanced and non-sinusoidal in nature when the MMC is not connected to the network. The reactive power compensation by MMC can be observed in Figure 8. The controller follows the reference reactive power $Q_{ref.}$ At time T = 5 seconds, the Q_{ref} changes from 50MVAR to 0MVAR. This leads to a dip in the power factor of the system measured at the Network Voltage. Figure 9 shows the active power compensation capability of the MMC. At T = 5 Seconds, the MMC stops supporting the grid to deliver Active Power to the load, which leads to an increase in Grid Current.

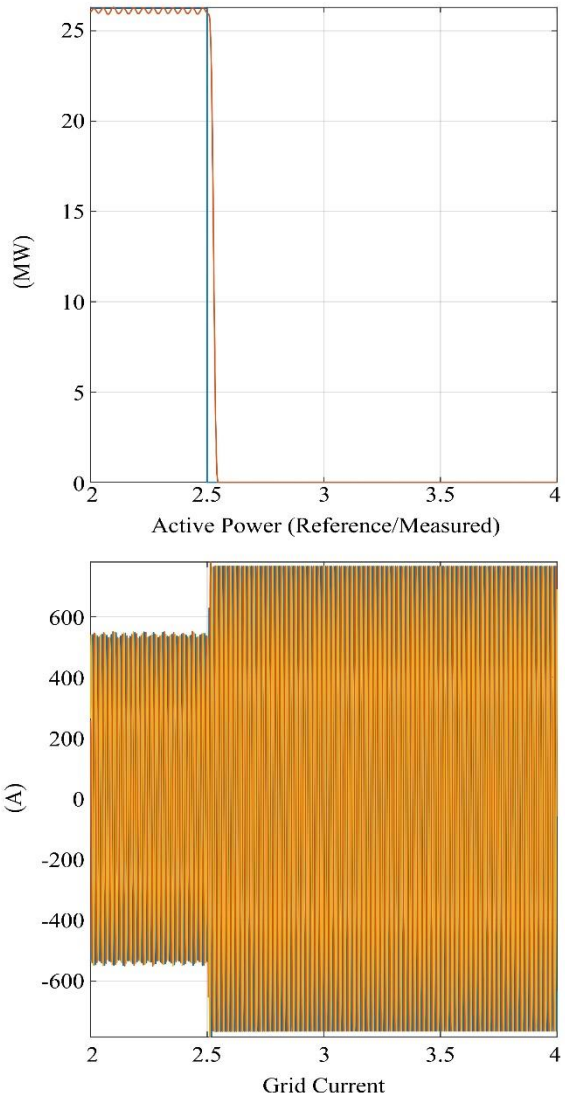

Fig. 9 Active power compensation with constant Q, Grid current

Table 3. Effect of MMC on the electrical network

Parameter	Without MMC	With MMC
Current harmonics	15%	1%
Flicker	5%	2%
Power factor	0.4	0.99
Additional support for the grid	No	Yes

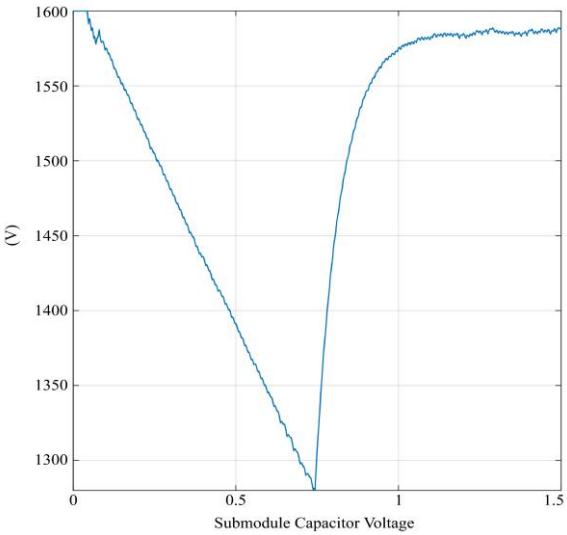

Fig. 10 Charging and discharging of submodule capacitors

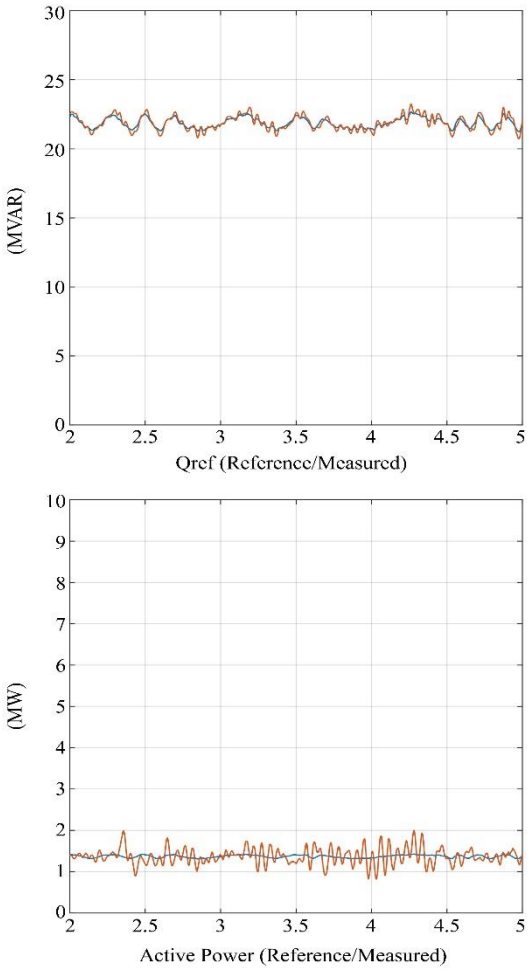

Fig. 11 Active and reactive power compensation with dynamic power measurement with measurement delay

The submodule capacitor voltage, during active power compensation, can be observed in Figure 10. When the capacitor voltage falls below 80% of the rated voltage, the submodule is connected with a DC voltage source like solar PV panels. The reactive power demand of the Electric Arc Furnace can vary frequently over time. In this case, the MMC is operated with a dynamically varying Q_{ref}. Voltage and current sensors are mounted at the load terminals to detect the active and reactive power demand of the EAF. However, voltage and current sensors have a measurement delay in the order of milliseconds [18]. Figure 11 shows the response of the controller with and without the instrument measurement delay of 0.7ms. For delays higher than 0.7ms, the controller needs to be updated with predictive methodologies for reference reactive power and active power.

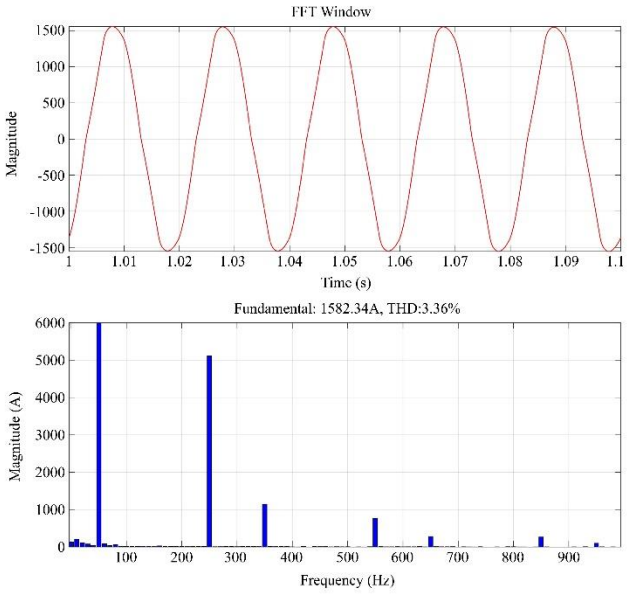

Fig. 12 FFT of grid current waveform without MMC

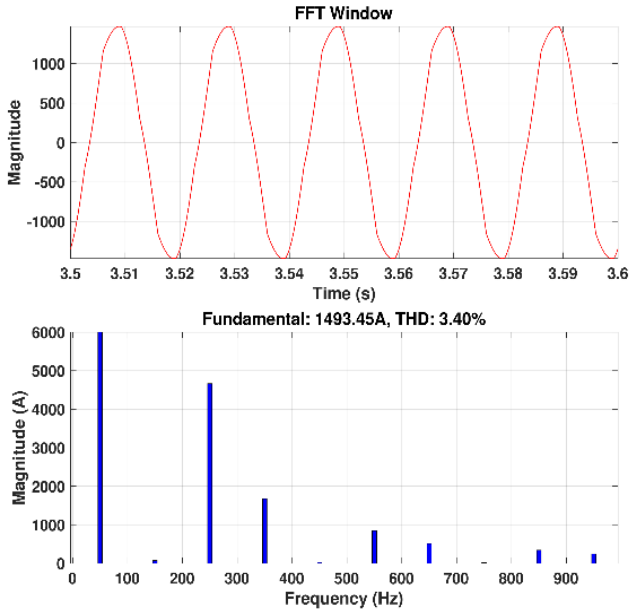

Fig. 13 FFT of grid current waveform while MMC is in operation

5. Conclusion

Due to the presence of an arc furnace, flickers are introduced in the load voltage, and harmonics are included in the load current. We can observe that MMC can mitigate the harmonics in the current waveform as seen in Figures 12 and 13. Therefore, the MMC-based solution is observed to be suitable for power quality improvement and visible flicker reduction in weak grids that supply power to large polluting loads like an Electric Arc Furnace. As seen in Section IV, the MMC-based STATCOM supports the weak grid by compensating for reactive power according to load demand and active power support to the grid.

References

[1] J. Sousa et al., "Harmonics and Flicker Analysis in Arc Furnace Power Systems," *Proceedings of the International Conference on Power Systems Transients (IPST)*, pp. 626-630, 1999. [Google Scholar] [Publisher Link]

[2] Ashutosh Srivastava, and Amarjeet Singh, "Harmonics Generated by Electric Arc Furnace in Electric Power System-A Review," *SAMRIDDHI A Journal of Physical Sciences, Engineering and Technology*, vol. 11, no. 1, pp. 57-62, 2019. [CrossRef] [Google Scholar] [Publisher Link]

[3] Giacomo Andrioli et al., "Modular Multilevel Converters for Next-Generation Electric Arc Furnaces in Steelmaking Electrification," *2023 IEEE Energy Conversion Congress and Exposition (ECCE)*, Nashville, TN, USA, pp. 6592-6594, 2023. [CrossRef] [Google Scholar] [Publisher Link]

[4] Ming Liu, Zetao Li, and Xiaoliu Yang, "A Universal Mathematical Model of Modular Multilevel Converter with Half-Bridge," *Energies*, vol. 13, no. 17, pp. 1-18, 2020. [CrossRef] [Google Scholar] [Publisher Link]

[5] Suman Debnath et al., "Operation, Control, and Applications of the Modular Multilevel Converter: A Review," *IEEE Transactions on Power Electronics*, vol. 30, no. 1, pp. 37-53, 2015. [CrossRef] [Google Scholar] [Publisher Link]

[6] M.A. Golkar, and S. Meschi, "MATLAB Modeling of Arc Furnace for Flicker Study," *2008 IEEE International Conference on Industrial Technology*, Chengdu, China, pp. 1-6, 2008. [CrossRef] [Google Scholar] [Publisher Link]

[7] B. Boulet, G. Lalli, and M. Ajersch, "Modeling and Control of an Electric Arc Furnace," *Proceedings of the 2003 American Control Conference*, Denver, CO, USA, vol. 4, pp. 3060-3064, 2003. [CrossRef] [Google Scholar] [Publisher Link]

[8] Johannes Gerhardt Bekker, Ian Keith Craig, and Petrus Christiaan Pistorius, "Modeling and Simulation of an Electric Arc Furnace Process," *ISIJ International*, vol. 39, no. 1, pp. 23-32, 1999. [CrossRef] [Google Scholar] [Publisher Link]

[9] Rodney H.G. Tan, and Vigna K. Ramachandaramurthy, *A Comprehensive Modeling and Simulation of Power Quality Disturbances using MATLAB/SIMULINK*, Power Quality Issues in Distributed Generation, IntechOpen, pp. 83-107, 2015. [CrossRef] [Google Scholar] [Publisher Link]

[10] Hani Saad et al., "Modelling of MMC Including Half-Bridge and Full-Bridge Submodules for EMT Study," *2016 Power Systems Computation Conference (PSCC)*, Genoa, Italy, pp. 1-7, 2016. [CrossRef] [Google Scholar] [Publisher Link]

[11] Chang Jiang, and Shaohua Zhang, "Power Quality Compensation Strategy of MMC-UPQC based on Passive Sliding Mode Control," *IEEE Access*, vol. 11, pp. 3662-3679, 2022. [CrossRef] [Google Scholar] [Publisher Link]

[12] Fazal Muhammad et al., "Design and Control of Modular Multilevel Converter for Voltage Sag Mitigation," *Energies*, vol. 15, no. 5, pp. 1-26, 2022. [CrossRef] [Google Scholar] [Publisher Link]

[13] Kamran Hafeez et al., "Circulating Current Reduction in MMC-HVDC System using Average Model," *Applied Sciences*, vol. 9, no. 7, pp. 1-24, 2019. [CrossRef] [Google Scholar] [Publisher Link]

[14] Mohammad Mirzaie Banafsh Tappeh, Javad Shokrollahi Moghani, and Amir Khorsandi, "Active and Reactive Power Control Strategy of the Modular Multilevel Converter for Grid-Connected Large Scale Photovoltaic Conversion Plants," *2019 10th International Power Electronics, Drive Systems and Technologies Conference (PEDSTC)*, Shiraz, Iran, pp. 309-314, 2019. [CrossRef] [Google Scholar] [Publisher Link]

[15] Mattia Ricco et al., "A Capacitor Voltage Balancing Approach Based on Mapping Strategy for MMC Applications," *Electronics*, vol. 8, no. 4, pp. 1-17, 2019. [CrossRef] [Google Scholar] [Publisher Link]

[16] Estíbaliz Solas et al., "Modular Multilevel Converter with Different Submodule Concepts-Part I: Capacitor Voltage Balancing Method," *IEEE Transactions on Industrial Electronics*, vol. 60, no. 10, pp. 4525-4535, 2013. [CrossRef] [Google Scholar] [Publisher Link]

[17] Shunliang Wang et al., "Capacitor Voltage Balancing Control with Reducing the Average Switching Frequency in MMC," *The Journal of Engineering*, vol. 2019, no. 16, pp. 2375-2380, 2019. [CrossRef] [Google Scholar] [Publisher Link]

[18] Imran Mohammed et al., "Modified Re-Iterated Kalman Filter for Handling Delayed and Lost Measurements in Power System State Estimation," *IEEE Sensors Journal*, vol. 20, no. 7, pp. 3946-3955, 2020 [CrossRef] [Google Scholar] [Publisher Link]